View metadata, citation and similar papers at core.ac.uk

brought to you by CORE

provided by Elsevier - Publisher Connector

Biophysical Journal Volume 76 May 1999 2421–2431

Quantifying Aggregation of IgE-FcεRI by Multivalent Antigen

William S. Hlavacek,* Alan S. Perelson,* Bernhard Sulzer,* Jennifer Bold,# Jodi Paar,# Wendy Gorman,§ and Richard G. Posner#

*Theoretical Biology and Biophysics, Los Alamos National Laboratory, Los Alamos, New Mexico 87545 and the Departments of #Chemistry and §Biology, Northern Arizona University, Flagstaff, Arizona 86011 USA

ABSTRACT Aggregation of cell surface receptors by multivalent ligand can trigger a variety of cellular responses. A well-studied receptor that responds to aggregation is the high affinity receptor for IgE (FcεRI), which is responsible for initiating allergic reactions. To quantify antigen-induced aggregation of IgE-FcεRI complexes, we have developed a method based on multiparameter flow cytometry to monitor both occupancy of surface IgE combining sites and association of antigen with the cell surface. The number of bound IgE combining sites in excess of the number of bound antigens, the number of bridges between receptors, provides a quantitative measure of IgE-FcεRI aggregation. We demonstrate our method by using it to study the equilibrium binding of a haptenated fluorescent protein, 2,4-dinitrophenol-coupled B-phycoerythrin (DNP_{25}-PE), to fluorescein isothiocyanate-labeled anti-DNP IgE on the surface of rat basophilic leukemia cells. The results, which we analyze with the aid of a mathematical model, indicate how IgE-FcεRI aggregation depends on the total concentrations of DNP_{25}-PE and surface IgE. As expected, we find that maximal aggregation occurs at an optimal antigen concentration. We also find that aggregation varies qualitatively with the total concentration of surface IgE as predicted by an earlier theoretical analysis.

INTRODUCTION

Aggregation of cell surface receptors is a common mechanism involved in signal transduction across a cell membrane (Metzger, 1992). This mechanism is used, for example, by receptors that are intrinsic protein tyrosine kinases (Pazin and Williams, 1992; Fry et al., 1993), such as the epidermal growth factor receptor (Schreiber et al., 1982) and the platelet derived growth factor receptor (Heldin et al., 1989), and by multichain immune recognition receptors (Keegan and Paul, 1992), such as the high affinity receptor for IgE (FcεRI) (Holowka and Baird, 1996) and the B-cell receptor (Kaye et al., 1983; Kaye and Janeway, 1984; Cambier and Ransom, 1987). For many of these receptors, early steps in the initiation of a signal are similar: multivalent interactions with a ligand lead to the aggregation of receptors and enhanced phosphorylation of tyrosines, which can be recognized by cytoplasmic regulatory molecules. The FcεRI receptor, for example, is triggered when IgE-FcεRI complexes are aggregated by multivalent antigen. Aggregation of FcεRI, which is constitutively associated with the protein tyrosine kinase Lyn (Eiseman and Bolen, 1992), then leads to a series of events, which include recruitment of additional Lyn kinases (El-Hillal et al., 1997; Wofsy et al., 1997).

Signals generated by aggregation of FcεRI, which can be negative or positive, depend on various properties of the aggregate structures that are formed on the cell surface. These properties include the overall number of receptors in aggregates on the cell surface, the size of aggregates (Fewtrell and Metzger, 1980; MacGlashan et al., 1983), the spacing of receptors in aggregates (Kane et al., 1986), and the time that individual receptors spend in aggregates (Torigoe et al., 1998). For example, it has been observed that IgE dimers are less effective than larger IgE oligomers at stimulating cellular responses (Fewtrell and Metzger, 1980) and that cellular responses are inhibited when an optimal degree of aggregation is exceeded (Becker et al., 1973; Menon et al., 1984; Seagrave and Oliver, 1990). Dependency of cellular responses on properties of receptor aggregates also has been observed for related receptors, such as the B-cell receptor (Dintzis et al., 1976, 1983) and T-cell receptor (Sloan-Lancaster et al., 1994; Madrenas et al., 1995; Lyons et al., 1996; Neumeister Kersh et al., 1998).

Because properties of ligand-induced receptor aggregates influence the signals that these aggregates generate, significant effort has been devoted to quantitative analysis of interactions between multivalent ligands and cell surface receptors, particularly in work with FcεRI (Goldstein, 1988; Goldstein and Wofsy, 1994). A goal of these studies has been to measure or predict the number of receptors in aggregates on the cell surface so that this quantity then can be compared and correlated with cellular responses (Dembo et al., 1978, 1979; Dembo and Goldstein, 1980; MacGlashan and Lichtenstein, 1983; MacGlashan et al., 1985). The number of receptors in aggregates is related to the number of receptor sites in aggregates, which in turn is related to the number of bound receptor sites in excess of the number of bound ligands. This difference, which can be interpreted as the number of receptor pairs in clusters (Perelson, 1981), is zero when ligand binding is monovalent and positive when

Received for publication 9 December 1997 and in final form 11 January 1999.

Address reprint requests to Dr. Alan S. Perelson, T-10, MS K710, Los Alamos National Laboratory, Los Alamos, NM 87545. Tel.: 505-667-6829; Fax: 505-665-3493; E-mail: asp@lanl.gov.

Reprint requests may also be addressed to Dr. Richard G. Posner, Department of Chemistry, Northern Arizona University, Flagstaff, AZ 86011. Tel.: 520-523-4209; Fax: 520-523-8111; E-mail: richard.posner@nau.edu.

© 1999 by the Biophysical Society

0006-3495/99/05/2421/11 $2.00

ligand binding is multivalent because each bound ligand must engage at least one receptor site. Thus, we can quantify receptor aggregation if we can measure ligand and receptor site binding.

One method to determine both the number of ligands bound to receptors and the occupancy of receptor sites involves differentially labeled monovalent and multivalent ligands. This method has been used in experiments with chemically cross-linked oligomers of IgE. For example, by incubating rat basophilic leukemia (RBL) cells, which express FcεRI, with ^{125}I-labeled dimers of IgE and then by adding ^{131}I-labeled IgE to assay the number of Fc receptor sites left unbound by IgE dimers, one can determine the number of Fc receptor sites in dimer-induced aggregates (Segal et al., 1977). This method works well with IgE oligomers, because IgE-FcεRI complexes are long lived (Kulczycki and Metzger, 1974; Sterk and Ishizaka, 1982). On the time scale of an experiment, the equilibrium between oligomeric IgE and FcεRI is undisturbed by monomeric IgE. However, the method is difficult to apply when receptor sites have low affinity for sites on the multivalent ligand, as in a typical physiological situation, because introduction of monovalent ligand can now rapidly influence binding of the multivalent ligand to receptors.

Here, we develop a method that can be used to measure simultaneously the amount of multivalent ligand bound to receptors and the occupancy of receptor sites without the complication of introducing a monovalent ligand. The method combines approaches previously used to measure the amount of ligand bound to receptors (Seagrave et al., 1987) and the occupancy of receptor sites (Erickson et al., 1986). To demonstrate the method, we study the equilibrium binding of haptenated phycoerythrin to anti-hapten IgE, which is labeled with fluorescein isothiocyanate (FITC). By using two-color flow cytometry to measure fluorescence of phycoerythrin and FITC, we are able to estimate the amount of antigen on the surface of RBL cells and the occupancy of surface IgE combining sites. These measurements also allow us to estimate the number of FcεRI pairs in antigen-induced clusters, i.e., the extent of receptor cross-linking.

Estimates of cross-linking are refined with the aid of a mathematical model, which we fit to data. The data are consistent with a model that accounts for cooperative effects, which arise, at least in part, for steric reasons. The model, which reduces to an equivalent site model (Perelson, 1981, 1984; Macken and Perelson, 1985; Lauffenburger and Linderman, 1993; Sulzer and Perelson, 1996) in the absence of cooperative effects, allows us not only to refine our estimates of cross-linking but also to determine equilibrium binding parameters. Furthermore, the development of this model, together with the ability to test its predictions against experimental measurements of both ligand binding and receptor site binding, provide new insights into methods for quantifying multivalent ligand-receptor interactions.

MODEL

To aid in analysis of experimental data, we develop a model for equilibrium binding of 2,4-dinitrophenol-coupled B-phycoerythrin (DNP_{25}-PE) to anti-DNP IgE-FcεRI complexes on RBL cells. In this model, we treat IgE-FcεRI as a bivalent cell surface receptor: each antibody combining site in an IgE-FcεRI complex represents one of two potential binding sites per receptor for the ligand, DNP_{25}-PE.

Reaction scheme

The model is based on the reaction scheme shown in Fig. 1 *A* in which ligands bind and aggregate receptor sites through a series of reversible reactions. The initial reaction involves the binding of solution-phase ligand to a receptor site, and each subsequent reaction involves the addition of a receptor site to a ligand-receptor complex (Fig. 1 *B*). In this scheme, ligand-receptor complexes form without intramolecular rearrangement reactions, i.e., without either ring or network formation reactions (Perelson, 1984; Macken and Perelson, 1985). If these reactions were significant, then the scheme in Fig. 1 *A* would have to be modified.

As indicated, the model is developed in terms of ligand states. Thus, variables in the model include the concentration of ligand in solution, which is denoted as L_0, the surface density of ligand that is bound to i receptor sites, which is denoted as L_i, and the surface density of free receptor sites, which is denoted as S. Related variables include the total concentration of ligand, which is denoted as L_T, and the total surface density of receptor sites, which is denoted as S_T.

Equilibria

To characterize the equilibria for the reactions in Fig. 1 *A*, we write

$$(i + 1)L_{i+1} = (n - i)K_i S L_i \quad \text{for } i = 0, \ldots, n - 1 \qquad (1)$$

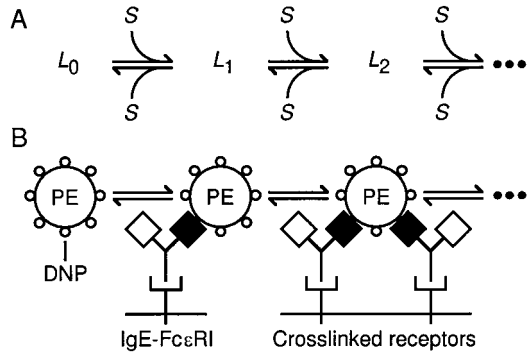

FIGURE 1 Reaction scheme. (*A*) Ligands bind receptor sites through a series of reversible reactions. L_0, L_1, L_2, and S indicate, respectively, a ligand in solution, a ligand bound to one receptor site, a ligand bound to two receptor sites, and a free receptor site. (*B*) A sequence of possible reactions is illustrated.

in which n is the chemical valence of the ligand (i.e., the number of DNP groups per PE molecule) and each K_i is an equilibrium constant. The equilibrium constant K_0 characterizes the affinity of a receptor site for a ligand site (i.e., a DNP group) when the ligand is in solution, and the cross-linking equilibrium constant K_i ($i \geq 1$) characterizes the affinity of a receptor site for a ligand site when the ligand is bound to i receptor sites (Dembo and Goldstein, 1978; Perelson, 1981). If K_1 through K_{n-1} are identical, Eq. 1 reduces to an equivalent site model (Perelson, 1981, 1984; Macken and Perelson, 1985; Lauffenburger and Linderman, 1993; Sulzer and Perelson, 1996).

Cooperativity

Sites on the ligand DNP_{25}-PE are chemically identical: each is a DNP group. Thus, the equilibrium constants in Eq. 1 are related, although K_1 through K_{n-1} need not be identical. Differences among these equilibrium constants indicate functional nonequivalence of ligand sites (i.e., cooperativity), which can arise for a variety of physical reasons (Perelson, 1984). Sites on DNP_{25}-PE are likely to be functionally nonequivalent, at least in part, for steric reasons. The crystal structure of B-phycoerythrin (Ficner et al., 1992; Ficner and Huber, 1993) indicates that this molecule is cylindrical with a height of 6 nm and a diameter of 11 nm. Thus, the exposed surface area of DNP_{25}-PE is ~200 square nm, which is insufficient to allow binding of more than a few DNP sites because the area covered by a bound antibody Fab arm is at least 30 square nm (Poljak et al., 1973; Padlan, 1994).

To account for functional nonequivalence of sites on DNP_{25}-PE, we introduce a cooperativity function $\phi(i)$ to relate the cross-linking equilibrium constants K_1 through K_{n-1} (Cantor and Schimmel, 1980):

$$K_i = e^{-\phi(i)} K_1 \quad \text{for } i = 1, \ldots, n-1 \tag{2}$$

in which $\phi(1) = 0$. The functional form of $\phi(i)$ is chosen to indicate how cooperative effects are expected to influence binding as a function of ligand site occupancy. If $\phi(i) = 0$ for all i, sites are functionally equivalent and K_1 through K_{n-1} are identical. However, for steric reasons, we can expect the value of the cross-linking equilibrium constant K_i to approach zero as i approaches the effective valence of DNP_{25}-PE, which we expect to be much less than the chemical valence n. This suggests that we should specify $\phi(i)$ as an increasing function of i. The simplest such form for $\phi(i)$, with the required property that $\phi(1) = 0$, is $a(i - 1)$, in which a is a positive constant.

Conservation

Because experiments are performed under conditions that inhibit recycling of FcεRI, we treat the total numbers of ligands and receptor sites as conserved quantities. Conservation of ligand can be expressed as

$$L_T = L_0 + C \sum_{i=1}^{n} L_i \tag{3}$$

in which L_T is the total concentration of ligand and C is a factor that converts surface densities to concentrations. This factor is the cell concentration, expressed in the same units as L_T, if each surface density L_i is expressed in units of ligand molecules per cell. Conservation of receptor sites can be expressed as

$$S_T = S + \sum_{i=1}^{n} iL_i \tag{4}$$

in which S_T is the total surface density of receptor sites, which is twice the total surface density of receptors.

Cross-linking

Ligand-induced aggregation of receptors is quantified by the number of cross-links on the cell surface. A cross-link is defined as follows (Perelson, 1981). In the absence of intramolecular rearrangement reactions, as in the scheme of Fig. 1 *A*, a ligand bound at i sites is attached to i receptors. Thus, a ligand bound at two sites, as depicted in Fig. 1 *B*, forms a single cross-link, i.e., a cluster of two receptors. If we generalize this concept of a cross-link, then a ligand bound at i sites forms $i - 1$ cross-links, i.e., $i - 1$ clusters of receptor pairs. Consequently, in the absence of intramolecular rearrangement reactions, the number of cross-links is given by $\sum_{i=1}^{n}(i - 1)L_i$, which is equivalent to the number of bound receptor sites ($\sum_{i=1}^{n} iL_i$) in excess of the number of bound ligands ($\sum_{i=1}^{n} L_i$).

MATERIALS AND METHODS

Reagents

Mouse monoclonal anti-DNP IgE was isolated from hybridoma H1 26.82 (Liu et al., 1980) by affinity purification (Holowka and Metzger, 1982). Final steps in the purification process included ion exchange chromatography to remove bound DNP-glycine, then gel filtration to separate monomeric IgE from small amounts of IgE aggregates. Fluorescently labeled IgE (FITC-IgE) was prepared by attaching fluorescein-5-isothiocyanate (Molecular Probes, Eugene, OR) to IgE (Erickson et al., 1986). The fluorescent antigen DNP_{25}-PE, which is composed of 2,4-dinitrophenol (DNP) and B-phycoerythrin (PE), was custom synthesized by Molecular Probes. The molar ratio of DNP to PE is 25:1. The molecular weight of DNP_{25}-PE is ~250,000.

Cells

RBL-2H3 cells (Barsumian et al., 1981) were grown adherent in 75 cm^2 flasks. Cell cultures, which were used typically 5 days after passage, were maintained at 37°C and 5% CO_2. Culture media consisted of MEM 1X with Earle's salts without glutamine (Gibco BRL), 20% fetal bovine serum (HyClone, Logan, UT), 1% v/v L-glutamine, 1% v/v penicillin, and 1% v/v streptomycin (Gibco BRL). To harvest cells, we rinsed and then incubated

the cells for 5 minutes at 37°C with trypsin-EDTA (Gibco BRL). Cells harvested for experiments were washed and resuspended in buffered salt solution (pH 7.7), which was freshly passed through a 0.22-μc filter. Buffered salt solution (BSS) consisted of 135 mM NaCl, 5 mM KCL, 1 mM $MgCl_2$, 1.8 mM $CaCl_2$, 5.6 mM glucose, 0.1% gelatin, and 20 mM Hepes. Cell suspensions in buffered salt solution were supplemented with 10 mM sodium azide and 10 mM 2-deoxy-D-glucose (Sigma, St. Louis, MO) to inhibit receptor recycling and cellular degranulation during binding experiments. To sensitize cells to DNP, we incubated cells overnight while cells were still in culture with excess (10 μg) anti-DNP FITC-IgE. Sensitized cells were exposed to FITC-IgE for at least 12 h prior to harvesting.

Flow cytometric binding assays

In each binding experiment, we incubated a suspension of sensitized cells at a density of 2.5×10^5, 10^6, or 4×10^6 cells/ml, with DNP_{25}-PE at room temperature. The concentration of DNP_{25}-PE varied from 0.0001 to 100 μg/ml. After cells were incubated with DNP_{25}-PE for at least 90 min, we used a Becton Dickinson FACScan flow cytometer, which was controlled with Cell Quest software, to collect histograms of FITC and PE fluorescence. We determined that 90 min was sufficient for binding to reach equilibrium at the relevant cell and ligand concentrations, because neither FITC nor PE fluorescence varied significantly as we varied the incubation time from 1 to 2 hours. Flow cytometric data were recorded as the mean FITC fluorescence (520 nm) of the cell suspension, FL1, and as the mean PE fluorescence (550 nm) of the cell suspension, FL2. To correct for nonspecific binding of DNP_{25}-PE to cells, we performed a control experiment in which cells lacked surface IgE. The difference between FL2 and the mean PE fluorescence for the control sample, ΔFL2, indicates the PE fluorescence due only to specific binding. To relate PE fluorescence to the surface density of DNP_{25}-PE, measurements of ΔFL2 were calibrated by using microspheres embedded with a known amount of B-phycoerythrin (Flow Cytometry Standards Corporation, San Juan, PR).

Data analysis

Relating measurements of fluorescence to binding

The fraction of surface IgE combining sites that are bound to DNP_{25}-PE, which we denote as σ, is related to variables in the model and, as established in earlier work (Erickson et al., 1986), to quenching of FITC-IgE fluorescence:

$$\sigma = 1 - S/S_T = \sum_{i=1}^{n} iL_i/S_T = (FL1_{max} - FL1)/(FL1_{max} - FL1_{min}) \quad (5)$$

in which FL1 is FITC fluorescence, $FL1_{max}$ is FL1 when all surface IgE combining sites are free ($\sigma = 0$), and $FL1_{min}$ is FL1 when all surface IgE combining sites are bound ($\sigma = 1$). In Eq. 5, the number of bound IgE combining sites $S_T - S$ is normalized by the total number of IgE combining sites S_T. Below, we also use S_T to normalize quantities that characterize DNP_{25}-PE binding and cross-linking, because neither the number of bound DNP_{25}-PE molecules nor the number of cross-links can be greater than the total number of IgE combining sites.

The ratio of cell-bound DNP_{25}-PE to surface IgE combining sites, which we denote as λ, is related to variables in the model and, as established in earlier work (Seagrave et al., 1987), to measurements of PE fluorescence:

$$\lambda = \sum_{i=1}^{n} L_i/S_T = \Delta FL2/\Delta FL2_{max} \quad (6)$$

in which ΔFL2 is PE fluorescence due to specific binding of DNP_{25}-PE to surface IgE and $\Delta FL2_{max}$ is ΔFL2 when DNP_{25}-PE binding is saturated, i.e., when each IgE combining site is bound to one molecule of DNP_{25}-PE ($\lambda = 1$).

Based on our earlier definition of a cross-link, the number of cross-links per IgE combining site, which we denote as χ, is related to σ and λ as follows:

$$\chi = \sum_{i=1}^{n}(i-1)L_i/S_T = \sum_{i=1}^{n} iL_i/S_T - \sum_{i=1}^{n} L_i/S_T = \sigma - \lambda \quad (7)$$

In the absence of intramolecular rearrangement reactions, χ indicates the normalized number of clustered IgE-FcϵRI pairs. In the presence of these reactions, χ is still related to cross-linking; however, in this case, χ is no longer directly proportional to the number of cross-links.

Estimating parameters by fitting the model to data

Three sets of data were used to determine best-fit values for K_0, K_1, S_T, and a, where a is a parameter in the specified cooperativity function $\phi(i)$. We considered various one-parameter functional forms for $\phi(i)$, including $\phi(i) = a(i-1)$. Each data set consisted of measurements of FITC fluorescence (FL1) and PE fluorescence (ΔFL2) for a series of ligand concentrations. These measurements were taken at one of three cell densities: 2.5×10^5, 10^6, or 4×10^6 cells/ml. Because data sets were collected with different instrument settings, it was necessary to determine best-fit scaling factors ($FL1_{min}$, $FL1_{max}$, and $\Delta FL2_{max}$) for each set of FL1 and ΔFL2 measurements.

Best-fit parameter values were determined by using the FORTRAN subroutine DNLS1 from the SLATEC Common Mathematical Library (http://www.netlib.org/slatec), which implements a modified Levenberg-Marquardt algorithm for solving nonlinear least-squares problems.

Solving the model equations

Equilibrium states are calculated by solving the model equations, which is aided by combining Eqs. 1–4. By using Eq. 1 to express each L_i as a function of S and L_0, by using Eq. 2 to relate K_1 through K_{n-1}, and by using Eq. 3 to express L_0 as a function of S, we can rewrite Eq. 4 to obtain

$$1 = S/S_T + \frac{K_0 L_T \sum_{i=1}^{n} i\pi(i)}{1 + K_0 C S_T \sum_{i=1}^{n} \pi(i)} \quad (8)$$

in which

$$\pi(i) = \binom{n}{i} \exp\left(-\sum_{j=0}^{i-1} \phi(j)\right)(K_1 S_T)^{i-1}(S/S_T)^i \quad (9)$$

Here, we adopt the convention that $\phi(0) = 0$. Cooperative effects are included entirely in the exponential term of Eq. 9. If this term reduces to 1, Eqs. 8 and 9 reduce to an equivalent site model.

When values for the parameters (n, C, L_T, S_T, K_0, and K_1) and a functional form for the cooperativity function $\phi(i)$ are specified, Eq. 8 is a nonlinear equation involving a single unknown: the fraction of free receptor sites S/S_T. To determine the fraction of free receptor sites at equilibrium, we solve this equation by using the method of bisection (Press et al., 1992). Once S/S_T is known, other states at equilibrium can be determined by using the relations $L_0/L_T = 1/[1 + K_0 C S_T \sum_{i=1}^{n} \pi(i)]$ and $L_i/S_T = (K_0 L_T)(L_0/L_T)\pi(i)$, which are derived from Eqs. 1–3.

RESULTS

We use multiparameter flow cytometry to study the equilibrium binding of a multivalent ligand to a cell surface receptor. The ligand, DNP_{25}-PE, is haptenated phycoerythrin (PE): each molecule of PE is coupled to an average of 25 DNP molecules. The receptor for this ligand is FITC-labeled anti-DNP IgE that is bound to FcεRI on the surface of RBL cells. Below, we first present qualitative features of DNP_{25}-PE binding to surface IgE, and we then illustrate how measurements of PE and FITC fluorescence can be used to quantify antigen-induced aggregation of IgE-FcεRI complexes. The methods developed here allow us to determine how equilibrium cross-linking varies quantitatively with the total concentrations of ligand and receptor.

Qualitative features of antigen binding to surface IgE

In our experiments, DNP_{25}-PE at various concentrations is added to suspensions of RBL cells that have been sensitized with FITC-IgE. Then, after equilibrium is reached, PE and FITC fluorescence are measured simultaneously in a flow cytometer. Fluorescence measurements for a series of experiments are shown in Fig. 2. As the concentration of DNP_{25}-PE increases, FITC fluorescence (FL1) decreases and PE fluorescence (ΔFL2) increases. A decrease in FITC fluorescence indicates an increase in the occupancy of IgE combining sites (Erickson et al., 1986), and an increase in PE fluorescence indicates an increase in association of DNP_{25}-PE with the cell surface (Seagrave et al., 1987).

Receptor binding saturates before ligand binding

As can be seen in Fig. 2, receptor sites saturate (i.e., FL1 reaches a lower plateau) at a ligand concentration of ~0.1 μg/ml, whereas ligand binding, as measured by ΔFL2, fails to reach an obvious plateau even at ligand concentrations greater than 10 μg/ml. This effect cannot be explained by nonspecific binding of ligand to cells, which was assayed in control experiments, because ΔFL2 represents the PE fluorescence due only to specific binding. We expect that ΔFL2 continues to rise after FL1 reaches a plateau for the following reason. When FL1 first reaches a plateau, ligand binding is multivalent. Then, as the ligand concentration increases, the multiplicity of ligand binding decreases, which allows more ligand to bind to the cell surface. As a result, ΔFL2 increases. This explanation is consistent with the binding parameters that we later determine.

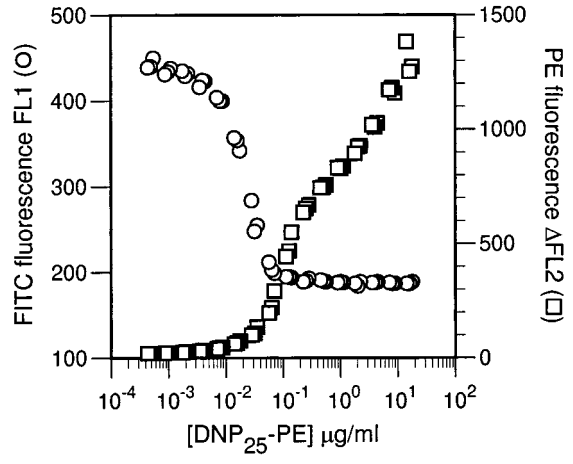

FIGURE 2 Flow cytometric measurements of PE and FITC fluorescence that monitor equilibrium binding of DNP_{25}-PE to FITC-IgE on the surface of RBL cells. The cell density is 10^6 cells/ml.

Ligand binding approaches saturation

At ligand concentrations greater than 20 μg/ml, measurements of PE fluorescence are unreliable due to light scatter. Thus, we are unable to measure PE fluorescence at saturation (i.e., we are unable to measure $\Delta FL2_{max}$) as is required to directly relate measurements of PE fluorescence to the extent of ligand binding (Eq. 6). Nevertheless, by using microspheres embedded with a known amount of PE to calibrate measurements of ΔFL2, we are able to estimate the extent of ligand binding. The calibration results indicate that the highest recorded value of ΔFL2 in Fig. 2 (1380) corresponds to $\sim 9 \times 10^5$ PE molecules per cell and at least the same number of receptor sites per cell (each bound ligand engages at least one receptor site). Thus, ligand binding approaches saturation in the experiments of Fig. 2 because RBL cells only express 300,000 to 600,000 FcεRI receptors per cell (Erickson et al., 1987). Based on this expected number of FcεRI receptors per cell, we can estimate that the highest recorded value of ΔFL2 is within at least 75% of $\Delta FL2_{max}$ because the minimum number of receptor sites per cell indicated by bead calibration (9×10^5) is 75% of the maximum number of surface IgE combining sites per RBL cell (1.2×10^6). As we will see later, model-based analysis indicates that ligand binding actually approaches 90% saturation in the experiments of Fig. 2.

Quantifying antigen-induced aggregation of surface IgE sites

We quantify receptor aggregation by determining the number of bound receptor sites in excess of the number of bound ligands. To determine this quantity, which we interpret as the number of cross-links, we must measure or estimate the scaling factors in Eqs. 5–7 ($FL1_{min}$, $FL1_{max}$, and $\Delta FL2_{max}$) and then use these equations to relate measurements of fluorescence (FL1 and ΔFL2) to quantities that characterize ligand and receptor binding (σ, λ, and χ).

Fluorescence measurements directly indicate a lower bound on cross-linking

The highest recorded value of ΔFL2 represents a lower bound on $\Delta FL2_{max}$. By using this lower bound, we can

place an upper bound on the extent of ligand binding and a lower bound on the extent of cross-linking, as can be seen by inspecting Eqs. 6 and 7. In Eq. 6, the number of bound ligands per receptor site λ is defined as $\Delta FL2/\Delta FL2_{max}$. Thus, an underestimate of $\Delta FL2_{max}$ leads to an overestimate of λ. In Eq. 7, the number of cross-links per receptor site χ is defined as $\sigma - \lambda$. Thus, an overestimate of λ leads to an underestimate of χ.

In Fig. 3, we show how the fluorescence measurements of Fig. 2 are related to biologically meaningful quantities. In Fig. 3 *A*, we plot receptor site occupancy σ, which is calculated by using Eq. 5, as a function of ligand concentration. The scaling factors $FL1_{min}$ and $FL1_{max}$, which appear in Eq. 5, are readily determined from the fluorescence data (Fig. 2). In Fig. 3 *B*, we plot the extent of ligand binding λ, which is calculated by using Eq. 6, as a function of ligand concentration. The values of λ were calculated by using the highest recorded value of ΔFL2 for $\Delta FL2_{max}$ in Eq. 6. Because we have determined only that this value is within 75% of $\Delta FL2_{max}$ (on the basis of our bead calibration results), values of λ are uncertain to the extent indicated by the error bars. However, as illustrated, the fluorescence data directly indicate an upper bound on ligand binding. In Fig. 3 *C*, we plot the extent of cross-linking χ, which is calculated by using Eq. 7, as a function of ligand concentration. As illustrated, an upper bound on λ translates to a lower bound on χ. Note that the increasing portion of the cross-linking curve is insensitive to the estimated uncertainty in $\Delta FL2_{max}$.

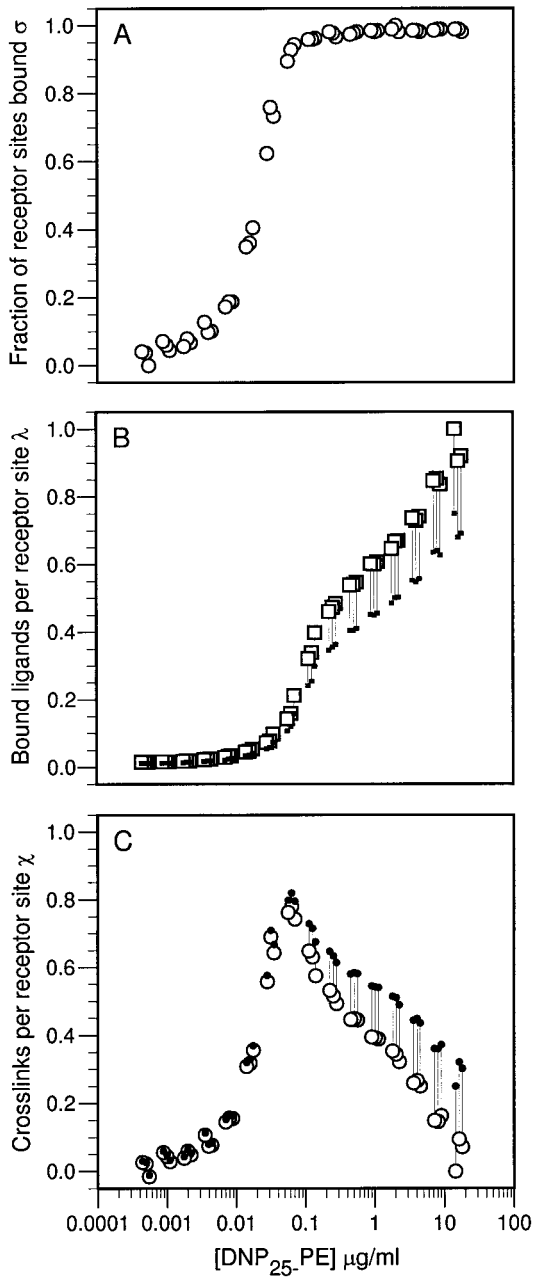

FIGURE 3 Equilibrium binding characterized by measurements of PE and FITC fluorescence. Fluorescence measurements directly indicate (*A*) the fraction of receptor sites bound σ, (*B*) an upper bound on the number of bound ligands per receptor site λ, and (*C*) a lower bound on the number of cross-links per receptor site χ. The points were derived from the fluorescence data in Fig. 2 by using Eqs. 5–7 and the scaling factors: $FL1_{min}$ = 184, the lowest recorded value of FL1, $FL1_{max}$ = 450, the highest recorded value of FL1, and $\Delta FL2_{max}$ = 1380, the highest recorded value of ΔFL2. The error bars in *B* and *C* indicate the uncertainty in λ and χ if the highest recorded value of ΔFL2 (1380) is within 75% of the actual $\Delta FL2_{max}$, as suggested by bead calibration. The small solid points at the end of error bars are based on $\Delta FL2_{max}$ = 1380/0.75. The cell density is 10^6 cells/ml.

Model-based analysis of fluorescence data yields refined estimates of receptor site occupancy, ligand binding, and cross-linking

To aid in the analysis of fluorescence data, we developed a model for ligand-receptor binding (Eqs. 1–4). We simultaneously fit this model to three data sets, one of which is that shown in Fig. 2. Each data set was collected at a different cell density. The following best-fit parameter values, which apply for all three data sets, were determined: $K_0 = 4.4 \times 10^8\ M^{-1}$, $K_1 S_T = 13$, and $S_T = 9.6 \times 10^5$ sites/cell. The fitting procedure also allowed us to specify $a = 0.43$ for the cooperativity function $\phi(i) = a(i - 1)$. We considered a variety of one-parameter functional forms for $\phi(i)$, but functions consistent with the data indicated essentially the same values for the cross-linking equilibrium constants K_1 through K_{n-1}. In addition to these parameter values, we also determined for each data set best-fit values for the scaling factors $FL1_{min}$, $FL1_{max}$, and $\Delta FL2_{max}$. For example, we determined that $\Delta FL2_{max}$ = 1500 for the data set of Fig. 2, which indicates that ligand binding in these experiments reached ~90% saturation (1380/1500).

The extent to which the model fits the data is illustrated in Fig. 4. Both the fraction of bound receptor sites and the number of bound ligands per receptor site are plotted as a function of ligand concentration. The points are derived from the fluorescence data of Fig. 2, Eqs. 5 and 6, and the best-fit scaling factors. These plots meet two expectations. First, the fraction of bound receptor sites σ is greater than or equal to the number of bound ligands per receptor site λ.

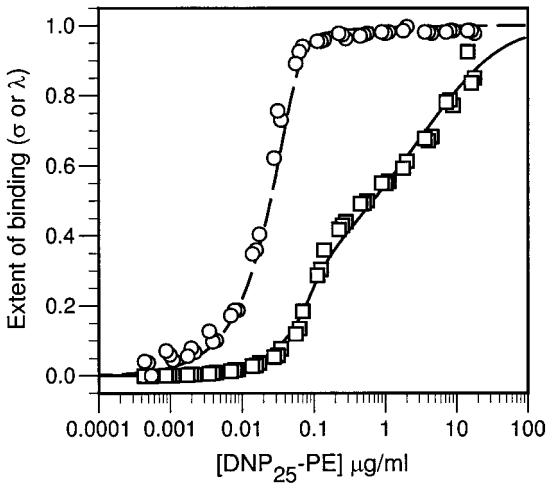

FIGURE 4 Comparison of best-fit theoretical binding curves with scaled data. The fraction of bound receptor sites σ (*circles*) and number of bound ligands per receptor site λ (*squares*) are plotted as a function of ligand concentration. The points were derived from the fluorescence data in Fig. 2 by using Eqs. 5 and 6, $FL1_{min} = 184$, $FL1_{max} = 450$, and $\Delta FL2_{max} = 1500$. The broken and solid lines indicate the theoretical binding curves, which are based on the model equations (Eqs. 1–4), Eqs. 5 and 6, $n = 25$, $S_T = 9.6 \times 10^5$ sites/cell, $K_0 = 4.4 \times 10^8\ M^{-1}$, $K_1S_T = 13$, and $\phi(i) = 0.43\ (i - 1)$. The cell density is 10^6 cells/ml.

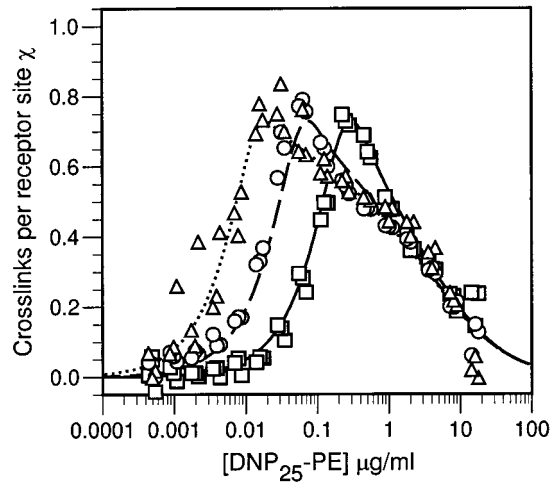

FIGURE 5 Best-fit estimates of cross-linking as a function of ligand concentration for three cell densities. The number of cross-links per receptor site χ is plotted as a function of ligand concentration for 2.5×10^5 cells/ml (*triangles*), 10^6 cells/ml (*circles*), and 4×10^6 cells/ml (*squares*). The points were derived from fluorescence data and best-fit scaling factors. For example, the points indicated by circles were derived from the fluorescence data in Fig. 2 by using Eqs. 5–7, $FL1_{min} = 184$, $FL1_{max} = 450$, and $\Delta FL2_{max} = 1500$. The lines indicate the theoretical binding curves, which are based on the model equations (Eqs. 1–4), Eq. 7, $n = 25$, $S_T = 9.6 \times 10^5$ sites/cell, $K_0 = 4.4 \times 10^8\ M^{-1}$, $K_1S_T = 13$, and $\phi(i) = 0.43\ (i - 1)$.

This result is expected because each bound ligand must engage at least one receptor site. Thus, σ must be greater than λ when ligand binding is multivalent, and σ must equal λ when ligand binding is monovalent. Second, σ and λ converge at high ligand concentrations, which indicates that ligand binding is predominantly monovalent at these concentrations. The quality of the fit illustrated in Fig. 4 is typical of the fits for the other two data sets.

The best-fit parameter values are consistent with independent data. The number of IgE combining sites per cell, 9.6×10^5, is consistent with our bead calibration results, which indicate 9×10^5 sites per cell, and with the number of FcεRI receptors (300,000 to 600,000 per cell) that are expressed on RBL cells (Erickson et al., 1987). The estimated affinity of anti-DNP IgE for DNP on haptenated PE, $4.4 \times 10^8\ M^{-1}$, is comparable with the affinity of anti-DNP IgE for DNP on haptenated bovine serum albumin, $8.5 \times 10^8\ M^{-1}$ (Xu et al., 1998). As expected, for steric reasons, the cooperativity function $\phi(i) = 0.43(i - 1)$ is an increasing function of ligand site occupancy i. Also, as is consistent with the structures of Fab and PE, theoretical values for the ratio σ/λ, which indicates the number of bound receptor sites per bound ligand molecule, are much less than the chemical valence of DNP_{25}-PE. For example, $\sigma/\lambda \approx 4$ at 0.1 μg/ml in Fig. 4 is where the cross-linking curve peaks (Fig. 5). Cross-linking is indicated by the vertical distance between the two curves in Fig. 4 because $\chi = \sigma - \lambda$ (Eq. 7).

The binding curves in Fig. 4, which are derived from our model-based analysis, can be compared with those in Fig. 3, which are derived directly from the fluorescence data. The two curves for receptor site binding are identical as can be seen by comparing Fig. 3 *A* with the corresponding plot in Fig. 4. The two curves for ligand binding also are similar. The binding curve in Fig. 4 falls within the range indicated in Fig. 3 *B* for ligand binding. In fact, this curve closely matches the upper bound on ligand binding indicated in Fig. 3 *B*. This suggests that our estimated upper bound on ligand binding and the resulting lower bound on cross-linking are tight and that the error bars shown in Fig. 3 overestimate the uncertainty in measurement of these quantities. The analysis-refined cross-linking curve that corresponds to Fig. 3 *C* is shown in Fig. 5.

Dependence of cross-linking on ligand and receptor concentration

In Fig. 5, we plot the extent of cross-linking χ as a function of ligand concentration for three cell densities. The points are derived from fluorescence measurements by using Eqs. 5–7 and best-fit scaling factors. Each curve indicates how cross-linking varies as a function of ligand concentration at a particular cell density or equivalently a particular receptor or receptor site concentration. Each of these cross-linking curves is bell shaped, as expected. Cross-linking increases with ligand concentration up to an optimal ligand concentration and then decreases as monovalent binding, because of excess ligand, begins to predominate.

The results shown in Fig. 5 indicate that cross-linking is influenced by the cell density. Three features are discernible. First, the location of the increasing portion of the cross-linking curve depends on the cell density. This portion

of the curve, which corresponds to the regime where receptor sites are not saturated, shifts to the right as the cell density increases. Thus, at a fixed ligand concentration, cross-linking decreases as the cell density increases if receptor site binding is below saturation. Second, the peak of the cross-linking curve is independent of cell density, i.e., each curve has the same maximum height. Third, the location of the decreasing portion of the cross-linking curve, which corresponds to the regime where receptor sites are saturated, tends not to depend on the cell density. As can be seen, the three curves coincide at ligand concentrations greater than 1 μg/ml. These qualitative features of cross-linking curves were predicted in an earlier theoretical analysis (Sulzer and Perelson, 1996).

DISCUSSION

In many antigen, hormone, and cytokine receptor systems, signal transduction is initiated by aggregation of cell surface receptors (Metzger, 1992). However, even in the well-studied FcϵRI system, the features of ligand-receptor binding that are critical for signaling have yet to be fully characterized, especially for cases in which the ligand has more than two binding sites. Here, we have developed and applied a flow cytometric method to monitor receptor site occupancy (Figs. 3 *A* and 4), ligand binding (Figs. 3 *B* and 4), and cross-linking (Figs. 3 *C* and 5). This study, like the recent work of Xu et al. (1998), represents an attempt to quantify the interactions of a multivalent antigen with IgE-FcϵRI.

The method that we have developed to quantify FcϵRI aggregation is significant for several reasons. First, the antigen is a haptenated protein (DNP_{25}-PE) that resembles a physiological allergen. Like an allergen, it elicits strong cellular responses (Seagrave et al., 1987). This is in contrast to bivalent haptens (Siraganian et al., 1975; Kane et al., 1986; Posner et al., 1995a). Also like an allergen, DNP_{25}-PE cross-links FcϵRI via antigen-antibody reactions. This is in contrast to oligomers of IgE; the kinetics of IgE binding to FcϵRI differ significantly from typical antigen-antibody kinetics (Kulczycki and Metzger, 1974; Sterk and Ishizaka, 1982). Second, the method allows us to characterize reactions on the cell surface without disturbing these reactions. This is in contrast to another flow cytometric method that recently has been developed to study multivalent ligand-receptor binding (Woodard et al., 1995). In this method, which we discuss later, a labeled monovalent ligand is used to determine the number of receptor sites that are bound by a differentially labeled multivalent ligand. Third, our method can be applied not only in equilibrium binding studies, as we have demonstrated here, but also in kinetic studies (Posner et al., 1998). Kinetic binding studies may be important for understanding the temporal properties of FcϵRI aggregates that influence signaling (MacGlashan et al., 1985; Torigoe et al., 1998).

We quantify receptor aggregation by determining two quantities: the number of bound receptor sites and the number of bound ligands. These quantities reveal information about the state of receptor aggregation. For example, if the number of bound ligands equals the number of bound receptor sites, then each ligand is bound to a single receptor site and no receptors are aggregated. In the absence of intramolecular rearrangement reactions, the number of bound receptor sites in excess of the number of bound ligands can be interpreted as the number of cross-links, i.e., the number of clustered receptor pairs (Perelson, 1981). We assume that this interpretation is valid here, i.e., we say that a cross-link is formed each time two receptor sites are joined. However, our use of this assumption does not represent a limitation of the method because cross-linking can be determined more directly if bispecific chimeric IgE is available. In experiments with this reagent, receptor aggregation is equivalent to receptor site aggregation, which is indicated by the number of bound receptor sites in excess of the number of bound ligands.

One approach that has been used to quantify FcϵRI aggregation involves oligomers of IgE (Segal et al., 1977). The number of bound oligomers is determined by radiolabeling. Monomeric IgE labeled with a different isotope is then used to determine the number of free FcϵRI receptors. Because dissociation of IgE from FcϵRI is slow (Kulczycki and Metzger, 1974; Sterk and Ishizaka, 1982), it is possible to add oligomeric IgE, reach equilibrium, and then add excess monomeric IgE to fill empty Fc sites without disturbing oligomer binding on the time scale of the experiment. Although oligomers of IgE are useful tools for studying receptor aggregation and subsequent cellular responses in this system, they have a number of limitations (Goldstein, 1988). Aggregates can be no larger than the number of chemically cross-linked IgE molecules, so IgE oligomers are unable to produce signals that depend on large receptor aggregates. Binding of IgE to FcϵRI is slow, so it may be difficult to separate the kinetics of oligomer binding from the kinetics of the cellular response. Also, IgE oligomers produce long-lived cross-links, and thus their effects may be atypical because signaling events that require the continual formation of new cross-links will not be observed.

Recently, Woodard et al. (1995) used a multivalent antigen to aggregate B-cell receptors and then used a differentially labeled monovalent antigen to count free receptor sites. Two-color flow cytometry was used together with FITC-DNP-L-papain, as a monovalent antigen, and TRITC-DNP-pol or TRITC-DNP-dextran, as a multivalent antigen, to determine the amount of monovalent antigen and the amount of multivalent antigen bound to DNP-specific B cells. Data obtained with this indirect method are difficult to interpret because the reactions are reversible (the typical dissociation rate constant for a bond between DNP and an antibody combining site is between 0.1 and 0.001 s^{-1}). Thus, on the time scale of these experiments, the binding of multivalent antigen is disturbed when the monovalent antigen is added to the system. In comparison, our method of measurement does not require an additional monovalent probe. Thus, it avoids the complications that arise when

different ligands compete for the same receptor. However, our approach requires that we label the receptors, which is impossible if the receptor is unavailable in a secreted form or cannot be reattached to the cell surface. The second condition is not fulfilled for many receptors, and consequently, an indirect method such as that used by Woodard et al. (1995) is then required to measure aggregation.

Another approach used to study FcεRI aggregation involves symmetric bivalent ligands, which represent the simplest type of ligand capable of aggregating receptors. Mathematical models have been developed for bivalent ligands interacting with bivalent cell surface receptors (Dembo and Goldstein, 1978; Perelson and DeLisi, 1980; Perelson, 1980; Wofsy and Goldstein, 1987; Posner et al., 1995b). However, a major limitation of these ligands is their inability to activate strong cellular responses. A variety of evidence suggests that these ligands are poor activators of cellular responses because they aggregate receptors predominantly in the form of stable cyclic dimers (Kane et al., 1986; Schweitzer-Stenner et al., 1987; Erickson et al., 1991; Posner et al., 1991; Posner et al., 1995a). Cyclic dimers, in which two ligand molecules connect two IgE-FcεRI complexes to form a closed ring, prevent chain elongation and limit the size of ligand-induced aggregates. With ligands of larger valence, such as DNP_{25}-PE, ring formation does not necessarily prevent growth of receptor aggregates. Thus, multivalent ligands are capable of cross-linking many IgE molecules and typically initiate strong cellular responses. When interacting with surface IgE, these ligands can form chain-, ring-, tree-, and network-like structures, whereas bivalent ligands can form only chain- and ring-like structures. This advantage of multivalent ligands is also a disadvantage, because a theory that describes the binding of multivalent ligands to bivalent receptors has yet to be fully developed. However, in a variety of related reaction systems studied in polymer chemistry, it has been found that ignoring the intramolecular reactions that form rings and networks leads to results that adequately characterize most aggregates (Flory, 1953), except those that form rubber-like materials. For these reasons, we have used a theory of multivalent ligand-receptor interactions that accounts for chain- and tree-like but not ring- and network-like aggregate structures. The model based on this theory is consistent with our binding data (Figs. 4 and 5).

In our efforts to estimate parameter values, we observed that unique best-fit parameter values are difficult to determine. To address this problem, we used three independent data sets, each collected at a different cell density and each consisting of both FL1 and ΔFL2 measurements. We obtain different results if we fit only FL1 data, only ΔFL2 data, or only data at a single cell density (unpublished material). This suggests that models of multivalent ligand-receptor interactions should be tested with a global analysis of multiple data sets (Posner and Dembo 1994; Myszka et al., 1998).

In summary, we have demonstrated a method by which the number of cross-links can be determined when both the number of receptor sites occupied and the number of ligands bound per receptor site are measured simultaneously. With this technique, we have confirmed that the equilibrium cross-linking curve is bell shaped (Figs. 3 *C* and 5). The results shown in Fig. 5 also confirm qualitative predictions concerning the influence of cell density on the cross-linking curve (Sulzer and Perelson, 1996). As predicted, we observe that an increase in cell density shifts the increasing portion of the cross-linking curve toward higher ligand concentrations, that the maximum height of the cross-linking curve is independent of cell density, and that the decreasing portion of the cross-linking curve also is independent of cell density. Thus, the equivalent site model studied by Sulzer and Perelson (1996) apparently can be used to predict the qualitative features of cross-linking curves for real ligands. However, to obtain quantitative estimates of binding parameters and more accurate quantification of ligand-receptor aggregation, it was important here to consider a more complicated model that included negative cooperativity due to steric effects. In conclusion, we have developed new theoretical and experimental tools for studying multivalent ligand-receptor binding.

We thank B. Goldstein for helpful discussions.

This work was performed under the auspices of the U.S. Department of Energy and was supported by Grants RR06555 and AI28433 to ASP and by Grant AI35997 to RGP from the National Institutes of Health.

REFERENCES

Barsumian, E. L., C. Isersky, M. G. Petrino, and R. P. Siraganian. 1981. IgE-induced histamine release from rat basophilic leukemia cell lines: isolation of releasing and nonreleasing clones. *Eur. J. Immunol.* 11: 317–323.

Becker, K. E., T. Ishizaka, H. Metzger, K. Ishizaka, and P. M. Grimley. 1973. Surface IgE on human basophils during histamine release. *J. Exp. Med.* 138:394–409.

Cambier, J. C., and J. T. Ransom. 1987. Molecular mechanisms of transmembrane signaling in B lymphocytes. *Annu. Rev. Immunol.* 5:175–199.

Cantor, C. R., and P. R. Schimmel. 1980. Biophysical Chemistry. Part III: The Behavior of Biological Macromolecules. Freeman, San Francisco. 859–862.

DeLisi, C. 1980. Theory of clustering of cell surface receptors by ligands of arbitrary valence: dependence of dose response patterns on a coarse cluster characteristic. *Math. Biosci.* 52:159–184.

Dembo, M., and B. Goldstein. 1978. Theory of equilibrium binding of symmetric bivalent haptens to cell surface antibody: application to histamine release from basophils. *J. Immunol.* 121:345–353.

Dembo, M., and B. Goldstein. 1980. A model of cell activation and desensitization by surface immunoglobulin: the case of histamine release from human basophils. *Cell*. 22:59–67.

Dembo, M., B. Goldstein, A. K. Sobotka, and L. M. Lichtenstein. 1978. Histamine release due to bivalent penicilloyl haptens: control by the basophil plasma membrane. *J. Immunol.* 121:354–358.

Dembo, M., B. Goldstein, A. K. Sobotka, and L. M. Lichtenstein. 1979. Histamine release due to bivalent penicilloyl haptens: relation of activation and desensitization of basophils to dynamic aspects of ligand binding to cell surface antibody. *J. Immunol.* 122:518–528.

Dintzis, H. M., R. Z. Dintzis, and B. Vogelstein. 1976. Molecular determinants of immunogenicity: the immunon model of immune response. *Proc. Natl. Acad. Sci. USA* 73:3671–3675.

Dintzis, R. Z., M. H. Middleton, and H. M. Dintzis. 1983. Studies on the immunogenicity and tolerogenicity of T-independent antigens. *J. Immunol.* 131:2196–2203.

Eiseman, E., and J. B. Bolen. 1992. Engagement of the high-affinity IgE receptor activates *src* protein-related tyrosine kinases. *Nature.* 355: 78–80.

El-Hillal, O., T. Kurosaki, H. Yamamura, J. P. Kinet, and A. M. Scharenberg. 1997. syk kinase activation by a src kinase-initiated activation loop phosphorylation chain reaction. *Proc. Natl. Acad. Sci. USA.* 94: 1919–1924.

Erickson, J., B. Goldstein, D. Holowka, and B. Baird. 1987. The effect of receptor density on the forward rate constant for binding of ligands to cell surface receptors. *Biophys. J.* 52:657–662.

Erickson, J., P. Kane, B. Goldstein, D. Holowka, and B. Baird. 1986. Crosslinking of IgE-receptor complexes at the cell surface: a fluorescence method for studying the binding of monovalent and bivalent haptens to IgE. *Mol. Immunol.* 23:769–781.

Erickson, J., R. Posner, B. Goldstein, D. Holowka, and B. Baird. 1991. Analysis of ligand binding and cross-linking of receptors in solution and on cell surfaces. Immunoglobulin E as a model receptor. *In* Biophysical and Biochemical Aspects of Fluorescence Spectroscopy. F. G. Dewey, editor. Plenum, New York. 169–195.

Fewtrell, C., and H. Metzger. 1980. Larger oligomers of IgE are more effective than dimers in stimulating rat basophilic leukemia cells. *J. Immunol.* 125:701–710.

Ficner, R., and R. Huber. 1993. Refined crystal structure of phycoerythrin from *Porphyridium cruentum* at 0.23-nm resolution and localization of the γ subunit. *Eur. J. Biochem.* 218:103–106.

Ficner, R., K. Lobeck, G. Schmidt, and R. Huber. 1992. Isolation, crystallization, crystal structure analysis and refinement of B-phycoerythrin from the red alga *Porphyridium sordidum* at 2.2 Å resolution. *J. Mol. Biol.* 228:935–950.

Flory, P. J. 1953. Principles of Polymer Chemistry. Cornell University Press, Ithaca, NY.

Fry, M. J., G. Panayotou, G. W. Booker, and M. D. Waterfield. 1993. New insights into protein-tyrosine kinase receptor signaling complexes. *Protein Sci.* 2:1785–1797.

Goldstein, B. 1988. Desensitization, histamine release and the aggregation of IgE on human basophils. *In* Theoretical Immunology, Part One. A. S. Perelson, editor. Addison-Wesley, Reading, MA. 3–40.

Goldstein, B., and C. Wofsy. 1994. Aggregation of cell surface receptors. *Lect. Math. Life Sci.* 24:109–135.

Heldin, C. H., A. Ernlund, C. Rorsman, and L. Ronnstrand. 1989. Dimerization of B-type platelet derived growth factor receptors occurs after ligand binding and is closely associated with receptor kinase activation. *J. Biol. Chem.* 264:8905–8912.

Holowka, D., and B. Baird. 1996. Antigen-mediated IgE receptor aggregation and signaling: a window on cell surface structure and dynamics. *Annu. Rev. Biophys. Biomol. Struct.* 25:79–112.

Holowka, D., and H. Metzger. 1982. Further characterization of the beta-component of the receptor for immunoglobulin E. *Mol. Immunol.* 19: 219–227.

Kane, P., J. Erickson, C. Fewtrell, B. Baird, and D. Holowka. 1986. Cross-linking of IgE-receptor complexes at the cell surface: synthesis and characterization of a long bivalent hapten that is capable of triggering mast cells and rat basophilic leukemia cells. *Mol. Immunol.* 23: 783–790.

Kaye, J., and C. A. Janeway, Jr. 1984. The Fab fragment of a directly activating monoclonal antibody that precipitates a disulfide-linked heterodimer from a helper T cell clone blocks activation by either allogeneic Ia or antigen and self-Ia. *J. Exp. Med.* 159:1397–1412.

Kaye, J., S. Porcelli, J. Tite, B. Jones, and C. A. Janeway, Jr. 1983. Both a monoclonal antibody and antisera specific for determinants unique to individual cloned helper T cell lines can substitute for antigen and antigen-presenting cells in the activation of T cells. *J. Exp. Med.* 158: 836–856.

Keegan, A. D., and W. E. Paul. 1992. Multichain immune recognition receptors: similarities in structure and signaling pathways. *Immunol. Today.* 13:63–68.

Kulczycki, A., Jr., and H. Metzger. 1974. The interaction of IgE with rat basophilic leukemia cells. II. Quantitative aspects of the binding reaction. *J. Exp. Med.* 140:1676–1695.

Lauffenburger, D. A., and J. J. Linderman. 1993. Receptors: Models for Binding, Trafficking, and Signaling. Oxford University Press, New York.

Liu, F. T., J. W. Bohn, E. L. Ferry, H. Yamamoto, C. A. Molinaro, L. A. Sherman, N. R. Klinman, and D. H. Katz. 1980. Monoclonal dinitrophenyl-specific murine IgE antibody: preparation, isolation, and characterization. *J. Immunol.* 124:2728–2737.

Lyons, D. S., S. A. Lieberman, J. Hampl, J. J. Boniface, Y. Chien, L. J. Berg, and M. M. Davis. 1996. A TCR binds to antagonist ligands with lower affinities and faster dissociation rates than to agonists. *Immunity.* 5:53–61.

MacGlashan, Jr., D., and L. M. Lichtenstein. 1983. Studies of antigen binding on human basophils. I. Antigen binding and functional consequences. *J. Immunol.* 130:2330–2336.

MacGlashan, Jr., D. W., M. Dembo, and B. Goldstein. 1985. Test of a theory relating to the cross-linking of IgE antibody on the surface of human basophils. *J. Immunol.* 135:4129–4134.

MacGlashan, Jr., D. W., R. P. Schleimer, and L. M. Lichtenstein. 1983. Qualitative differences between dimeric and trimeric stimulation of human basophils. *J. Immunol.* 130:4–6.

Macken, C. A., and A. S. Perelson. 1985. Branching Processes Applied to Cell Surface Aggregation Phenomena, Volume 58 of Lecture Notes in Biomathematics. Springer-Verlag, New York.

Madrenas, J., R. L. Wange, J. L. Wang, N. Isakov, L. E. Samelson, and R. N. Germain. 1995. Zeta phosphorylation without ZAP-70 activation induced by TCR antagonists or partial agonists. *Science.* 267:515–518.

Menon, A. K., D. Holowka, and B. Baird. 1984. Small oligomers of immunoglobulin E (IgE) cause large-scale clustering of IgE receptors on the surface of rat basophilic leukemia cells. *J. Cell. Biol.* 98:577–583.

Metzger, H. 1992. Transmembrane signaling: the joy of aggregation. *J. Immunol.* 149:1477–1487.

Myszka D. G., X. He, M. Dembo, T. A. Morton, and B. Goldstein. 1998. Extending the range of rate constants available from BIACORE: interpreting mass transport-influenced binding data. *Biophys. J.* 75:583–594.

Neumeister Kersh, E., A. S. Shaw, and P. M. Allen. 1998. Fidelity of T cell activation through multistep T cell receptor ζ phosphorylation. *Science.* 281:572–575.

Padlan, E. A. 1994. Anatomy of the antibody molecule. *Mol. Immunol.* 31:169–217.

Pazin, M. J., and L. T. Williams. 1992. Triggering signaling cascades by receptor tyrosine kinases. *Trends Biochem. Sci.* 17:374–378.

Perelson, A. S. 1980. Receptor clustering on a cell surface. II. Theory of receptor cross-linking by ligands bearing two chemically distinct functional groups. *Math. Biosci.* 49:87–110.

Perelson, A. S. 1981. Receptor clustering on a cell surface. III. Theory of receptor cross-linking by multivalent ligands: description by ligand states. *Math. Biosci.* 53:1–39.

Perelson, A. S. 1984. Some mathematical models of receptor clustering by multivalent ligands. *In* Cell Surface Dynamics: Concepts and Models. A. S. Perelson, C. DeLisi, and F. W. Wiegel, editors. Marcel Dekker, New York. 223–276.

Perelson, A. S., and C. DeLisi. 1980. Receptor clustering on a cell surface. I. Theory of receptor cross-linking by ligands bearing two chemically identical functional groups. *Math. Biosci.* 48:71–110.

Poljak, R. J., L. M. Amzel, H. P. Avey, B. L. Chen, R. P. Phizackerley, and F. Saul. 1973. Three-dimensional structure of the Fab′ fragment of human immunoglobulin at 2.8-Å resolution. *Proc. Natl. Acad. Sci. USA.* 70:3305–3310.

Posner, R. G., J. Bold, Y. Bernstein, J. Rasor, J. Braslow, W. S. Hlavacek, and A. S. Perelson. 1998. Measurement of receptor crosslinking at the cell surface via multiparameter flow cytometry. *SPIE.* 3256:132–143.

Posner, R. G., and M. Dembo. 1994. Binding of bivalent ligand to cell surface IgE: can one detect ring formation? *Mol. Immunol.* 31: 1439–1445.

Posner, R. G., J. W. Erickson, D. Holowka, B. Baird, and B. Goldstein. 1991. Dissociation kinetics of bivalent ligand immunoglobulin E aggregates in solution. *Biochemistry.* 30:2348–2356.

Posner, R. G., K. Subramanian, B. Goldstein, J. Thomas, T. Feder, D. Holowka, and B. Baird. 1995a. Simultaneous cross-linking by two nontriggering bivalent ligands causes synergistic signaling of IgE FcεRI complexes. *J. Immunol.* 155:3601–3609.

Posner, R. G., C. Wofsy, and B. Goldstein. 1995b. The kinetics of bivalent ligand-bivalent receptor aggregation: ring formation and the breakdown of the equivalent site approximation. *Math. Biosci.* 126:171–190.

Press, W. H., S. A. Teukolsky, W. T. Vetterling, and B. P. Flannery. 1992. Numerical Recipes in FORTRAN: The Art of Scientific Computing, 2nd edition. Cambridge University Press, New York.

Schreiber, A. B., T. A. Libermann, I. Lax, Y. Yarden, and J. Schlessinger. 1982. Biological role of epidermal growth factor receptor clustering: investigation with monoclonal anti-receptor antibodies. *J. Biol. Chem.* 258:846–853.

Schweitzer-Stenner, R., A. Licht, I. Luscher, and I. Pecht. 1987. Oligomerization and ring closure of immunoglobulin E class antibodies by divalent haptens. *Biochemistry.* 26:3602–3612.

Seagrave, J. C., G. G. Deanin, J. C. Martin, B. H. Davis, and J. M. Oliver. 1987. DNP-phycobiliproteins, fluorescent antigens to study dynamic properties of antigen-IgE-receptor complexes on RBL-2H3 rat mast-cells. *Cytometry.* 8:287–295.

Seagrave, J. C., and J. M. Oliver. 1990. Antigen-dependent transition of IgE to a detergent-insoluble form is associated with reduced IgE receptor-dependent secretion from RBL-2H3 mast cells. *J. Cell. Physiol.* 144:128–136.

Segal, D. M., J. D. Taurog, and H. Metzger. 1977. Dimeric immunoglobulin E serves as a unit signal for mast cell degranulation. *Proc. Natl. Acad. Sci. USA.* 74:2993–2997.

Siraganian, R. P., W. A. Hook, and B. B. Levine. 1975. Specific in vitro histamine release from basophils by bivalent haptens: evidence for activation by simple bridging of membrane bound antibody. *Immunochemistry.* 12:149–157.

Sloan-Lancaster, J., A. S. Shaw, J. B. Rothbard, and P. M. Allen. 1994. Partial T cell signaling: altered phospho-zeta and lack of zap70 recruitment in APL-induced T cell anergy. *Cell.* 79:913–922.

Sterk, A. R., and T. Ishizaka. 1982. Binding properties of IgE receptors on normal mouse mast cells. *J. Immunol.* 128:838–843.

Sulzer, B., and A. S. Perelson. 1996. Equilibrium binding of multivalent ligands to cells: effects of cell and receptor density. *Math. Biosci.* 135:147–185.

Torigoe, C., J. K. Inman, and H. Metzger. 1998. An unusual mechanism for ligand antagonism. *Science*. 281:568–572.

Wofsy, C., and B. Goldstein. 1987. The effect of co-operativity on the equilibrium binding of symmetric bivalent ligands to antibodies: theoretical results with application to histamine release from basophils. *Mol. Immunol.* 24:151–161.

Wofsy, C., C. Torigoe, U. M. Kent, H. Metzger, and B. Goldstein. 1997. Exploiting the difference between intrinsic and extrinsic kinases: implications for regulation of signaling by immunoreceptors. *J. Immunol.* 159:5984–5992.

Woodard, S. L., M. Aldo-Benson, D. A. Roess, and B. G. Barisas. 1995. Flow cytometric analysis of T-independent antigen binding to dinitrophenyl-specific cells. *J. Immunol.* 155:163–171.

Xu, K., B. Goldstein, D. Holowka, and B. Baird. 1998. Kinetics of multivalent antigen DNP-BSA binding to IgE-FcεRI in relationship to the stimulated tyrosine phosphorylation of FcεRI. *J. Immunol.* 160: 3225–3235.